

Sensitivity of CuS Membrane pH Sensor With and Without MOSFET

FAYROZ A. SABAH,^{1,2,6} NASER M. AHMED,^{1,7} Z. HASSAN,³
MUNIRAH ABDULLAH ALMESSIERE,⁴ and NAIF H. AL-HARDAN⁵

1.—School of Physics, Universiti Sains Malaysia, 11800 USM Penang, Malaysia. 2.—Department of Electrical Engineering, College of Engineering, Al-Mustansiriya University, Baghdad, Iraq. 3.—Institute of Nano Optoelectronics Research and Technology (INOR), Universiti Sains Malaysia, 11800 USM Penang, Malaysia. 4.—Physics Department, College of Science, University of Dammam, Dammam, Saudi Arabia. 5.—School of Physics, Faculty of Science and Technology, Universiti Kebangsaan Malaysia, 43600 Bangi, Malaysia. 6.—e-mail: fayroz_arif@yahoo.com. 7.—e-mail: naser@usm.my

Many studies have been conducted on membranes implemented as pH sensors for measuring pH sensitivity; nevertheless, the effect of metal oxide semiconductor field effect transistors was not taken into account. Hence, this study was conducted to measure the sensitivity of the CuS membrane with and without a field effect transistor. The CuS membrane was deposited onto a glass substrate using the spray pyrolysis technique. The sensitivity and linearity in the absence of the field effect transistor were measured to be 22.86 mV/pH and 95.62%, whereas the presence of the field effect showed slightly higher sensitivity and linearity of 24 mV/pH and 98.18%, respectively. The CuS membrane synthesized in the presence of the field effect transistor also showed higher stability because the metal oxide semiconductor was not immersed in a buffer solution. Furthermore, the hysteresis of the CuS membrane, measured for 5 min, yielded a value of 12.8 mV. The structural characteristics of the membrane confirmed the formation of a single, pure CuS phase, whereas the morphological characteristics showed porous agglomerations of square nanocrystals.

INTRODUCTION

Sensitivity detection entails the measurement of a change in the surface potential between the gate insulator and the electrolyte. This change in the surface potential modifies the electric field at the insulator–semiconductor interface and modulates the channel conductance that affects drain current. Because the channel conductance and drain current can be modulated, it is possible to measure the changes by applying a fixed source to the drain voltage. When this method is used, the gate voltage is typically plotted linearly against various pH values, which can be used to measure an unknown acid or an alkaline solution.¹ The first ion-sensitive field effect transistor (ISFET) was fabricated by Bergveld in the 1970s.² The difference between ISFET and a metal oxide semiconductor field effect transistor (MOSFET) is the presence of a metal gate electrode in the latter,³ which is directly exposed to a buffer solution.¹ Silicon dioxide (SiO₂) is the first

pH-sensitive membrane to be used for the ISFET.⁴ Over time, several other materials such as Al₂O₃, Si₃N₄, Ta₂O₅, and SnO₂ have been employed because of their higher pH response. For instance, Chi et al.³ measured the sensitivity of tin oxide (SnO₂) sensing membrane with and without MOSFET and deduced that the sensitivity with MOSFET (58 mV/pH) is slightly higher when compared with that without MOSFET (56 mV/pH).

An extended gate field effect transistor (EGFET) is a structure that isolates FET from the chemical environment, wherein a chemically sensitive membrane is deposited at the end of the signal line extended from the FET gate electrode. This structure has several benefits, such as insensitivity to light, simple-to-passive packaging, flexibility of shape of the extended gate area,³ and improved long-term stability.⁵ In addition, it is economical, easy to manufacture, highly responsive, exceptionally convenient, and stable under light and ambient temperature. These exceptional properties make the

EGFET structure ideal for use in disposable detection devices.⁶ Moreover, the approach of using a disposable membrane enables the swapping of the sensing membrane in case of chemical damage rather than fabricating a new device.⁷

Based on the site-binding model, the chemical sensitivity was found to be dependent on the total number of surface sites per unit area (N_S). Thus, the larger N_S should facilitate the ion sensing. Consequently, one-dimensional nanostructures such as nanowires, nanobelts, nanorods, and nanotubes attracted a lot of attention for pH sensing as a result of their high surface-to-volume ratio with larger effective sensing areas.⁸ With the development of robust sensors, there is a growing trend toward the use of disposable sensors in medical applications. Recently, biosensors and pH sensors have been used in the biomedical field.⁶ Copper sulfide (CuS) thin film attracts great attention as a result of its semiconducting properties, whereas its constituent elements (Cu and S) are nontoxic.⁹ In addition, CuS has become an alternative candidate in modifying wide bandgap semiconductors because it is eco-friendly and economic friendly.¹⁰

Furthermore, CuS thin film has been implemented in various applications that include solar cells,¹¹ gas sensors,¹² and photosensors.¹³ Nevertheless, based on a detailed literature review, CuS thin film has not been synthesized as an EGFET pH sensor with deionized water and spray pyrolysis at ambient light and room temperature. In this research work, CuS membrane was deposited by spray pyrolysis deposition (SPD) technique. The CuS membrane was applied as an EGFET in the fabrication of a pH sensor. The sensitivity of the CuS membrane was measured without and with MOSFET. The hysteresis of the membrane was also estimated.

EXPERIMENTAL PART

Thin Film Preparation

CuS thin film was synthesized via a spray pyrolysis deposition (SPD) technique comprising copper chloride (CuCl_2) and sodium thiosulfate ($\text{Na}_2\text{S}_2\text{O}_3$) as sources of Cu^{2+} and S^{2-} , respectively. First, the precursors were dissolved separately in deionized water. A 0.4-M concentration of each solution was then mixed with the other. The glass substrate was cleaned and dried prior to deposition. The deposition temperature was fixed at 200°C, whereas the distance between the nozzle and the substrate was set at 30 cm. After completing the deposition, the thin film was kept on a heater for 1 h to complete the growing process.

Characterization Techniques

A PANalytical x-ray diffractometer (XRD) equipped with $\text{CuK}\alpha$ source radiation ($\lambda = 0.15418$ nm) was used to check the phase

purity and crystal structure. NOVA NANOSEM 450 field emission scanning electron microscopy (FESEM) was used for morphological observations. For sensing measurements, a Keithley Semiconductor Characterization System (2400-SCS) was used to measure pH sensitivity.

pH-Sensing System Setup

The pH-sensing system is separated into two stages: the sensitivity of the membrane was measured without and with available MOSFET; see Fig. 1.

RESULTS AND DISCUSSION

Structural Analysis

In solid-state physics, solid-state chemistry, and material science, XRD is one of the most significant characterization techniques used by researchers to determine average grain size and the elastic properties of nanocrystals.¹⁴ Several peaks of the XRD spectra of as-deposited CuS membrane (Fig. 2a) were indexed to indicate the hexagonal structure of the covellite CuS phase (JCPDS card No. 06-0464), which confirms the formation of a single, pure CuS phase. Peak broadening with crystallite size (D) and lattice strain (ϵ) as a result of dislocation can be estimated by XRD.^{14,15}

Scherrer Method

The crystallite size is calculated from the full width at half maximum (FWHM) of the peaks (100), (102), (103), (006), (105), (008), and (110) with the Scherrer equation^{14,15} expressed as:

$$D = \frac{k\lambda}{\beta_D \cos \theta} \quad (1)$$

where k indicates the Scherrer constant (shape factor) usually taken around 0.9; λ symbolizes the wavelength of the incident $\text{Cu-K}\alpha$ radiation, typically equal to 0.154 nm; β denotes the broadening of diffraction line measured at half of its maximum intensity (in radian); and θ is the Bragg diffraction angle (in degree).¹⁴ The crystallite sizes calculated from Eq. 1 using miller indices (hkl), diffraction angle (2θ), measured peak broadening (β), and distance between adjacent planes (d_{hkl}) are listed in Table I. The combination of both instrument- and sample-dependent effects gives the breadth of the Bragg peak. Thus, the instrument-corrected broadening (β_D) corresponding to the diffraction peak of CuS was estimated with:¹⁴

$$\beta_{hkl}^2 = (\beta)_{\text{measured}}^2 - (\beta)_{\text{instrumental}}^2 \quad (2)$$

where $\beta_{\text{instrumental}}$ refers to the instrumental peak broadening; for all calculations, a standard silicon peak (111) was used to correct the instrumentation broadening effects. From Eq. 1, it is clear that peak width varies as $(1/\cos\theta)$.¹⁴ By applying Eqs. 1 and 2, the average crystallite size of the CuS nanoparticles was estimated to be 16.02 nm.

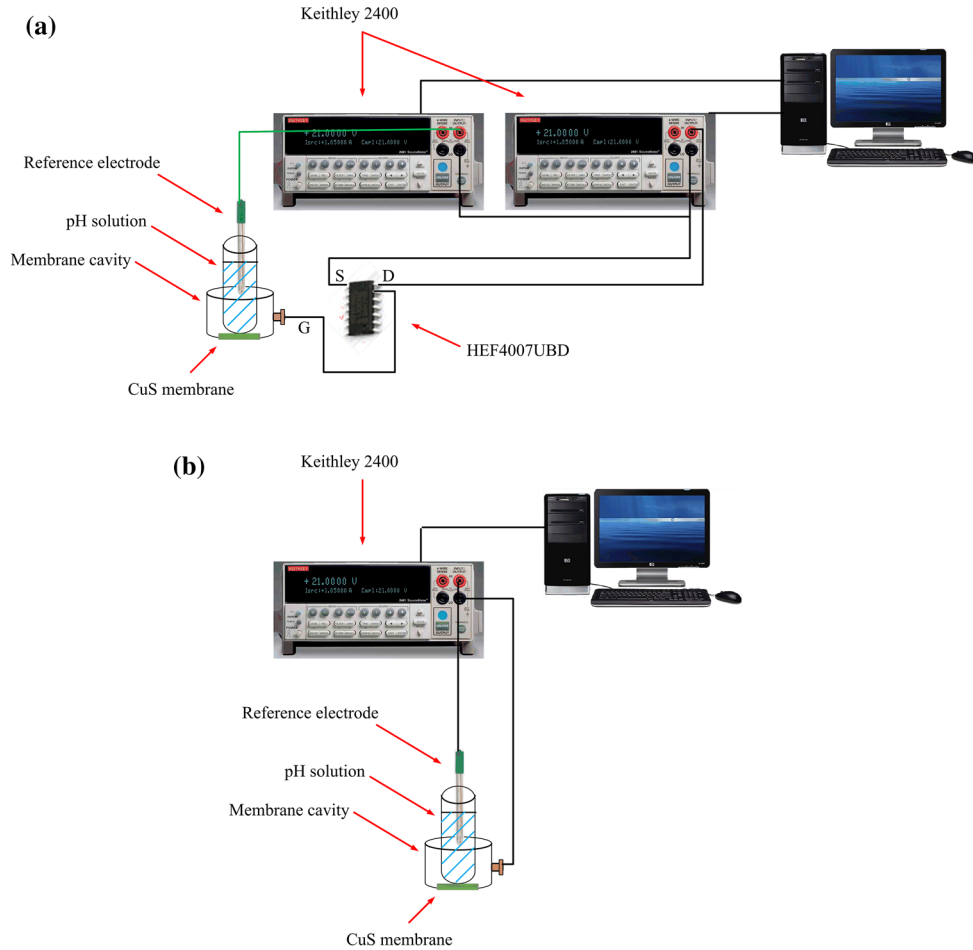


Fig. 1. pH sensitivity setup (a) with MOSFET (b) without MOSFET.

Williamson–Hall Method

The Williamson–Hall approach assumes that size and strain broadening are additive components of the total integral breadth of a Bragg peak.¹⁵ This method provides a plot (Hall plot) comprising a uniform deformation model (UDM), as shown in Fig. 2b. The strain-induced broadening in XRD as a result of crystal deformation and distortion was calculated with:^{14,15}

$$\varepsilon = \frac{\beta_{hkl}}{4 \tan \theta} \quad (3)$$

From Eq. 3, it is clear that the strain varies with $\tan \theta$.¹⁴ The Williamson–Hall method is the addition of Eq. 1 with the expression in Eq. 3, which can be expressed by:^{14,15}

$$\beta_{hkl} = \left(\frac{k\lambda}{D \cos \theta} \right) + (4\varepsilon \tan \theta) \quad (4)$$

When the Scherrer equation Eq. 4 are rearranged, the final form of the Williamson–Hall equation is expressed as:

$$\beta_{hkl} \cos \theta = \left(\frac{k\lambda}{D} \right) + (4\varepsilon \sin \theta) \quad (5)$$

A Hall plot was performed for CuS nanostructures for the orientation peaks with the hexagonal phase, as illustrated in Fig. 2b. The y-axis of this plot indicates $(\beta \cos \theta)$, and the x-axis represents $(4 \sin \theta)$. Accordingly, the slope and y-intersect of the fitted line represent strain and particle size, respectively. The following equation was used to estimate the slope and the y-intersect of the plot:

$$y = mx + c \quad (6)$$

where m represents the slope $(\Delta\beta \cos \theta / \Delta 4 \sin \theta)$, and c denotes y-intersect of the fitted data. m and c indicate the microstrain and crystallite size, respectively. From Eqs. 1 and 3, it is proven that peak broadening from crystallite size varies as $1/\cos \theta$, strain varies as $\tan \theta$. This essential difference that results when both microstructural causes—small crystallite size and microstrain—occur together allows for a secession of reflection broadening. Williamson and Hall separated size and strain broadening analysis according to various θ positions.^{14,15} The crystallite size according to the Williamson–Hall method was estimated to be 14.86 nm.

Morphological Observation

An FESEM image with an inset of EDX (Fig. 3) of the CuS membrane shows a nonhomogeneous morphology and random size distribution of square-shaped nanoparticles with the presence of pores. Aggregation of the nanostructured particles on some spots of the film surface is observed, which can be attributed to the dependence of SPD on

temperature and the disparity in thermal distribution. An EDX scan of the film surface depicts the presence of Cu and S, which are the precursor materials of the thin film. The average film thickness of approximately $3\ \mu\text{m}$ was estimated from several thickness readings in different areas. Both structural and morphological characteristics confirmed the CuS nanocrystalline hexagonal structure with a pure covellite phase, which is significant for improving the membrane properties of the pH sensor. The nanocrystalline structure with a smaller grain size has a large surface-to-volume ratio, which is a critical property for improving pH sensitivity as reported by Safaa et al.¹⁶ in their study on size reduction of ZnO to a nanocrystalline form and its vital role in improving pH sensing.

pH Sensitivity and Linearity

This section details the influence of nanostructured crystals on pH sensitivity improvement. Because the pH sensor depends on the surface reaction, the number of available sites (N_S) on the membrane surface (surface site density) in addition to the surface-to-volume ratio of the nanocrystallines are the most significant parameters that control

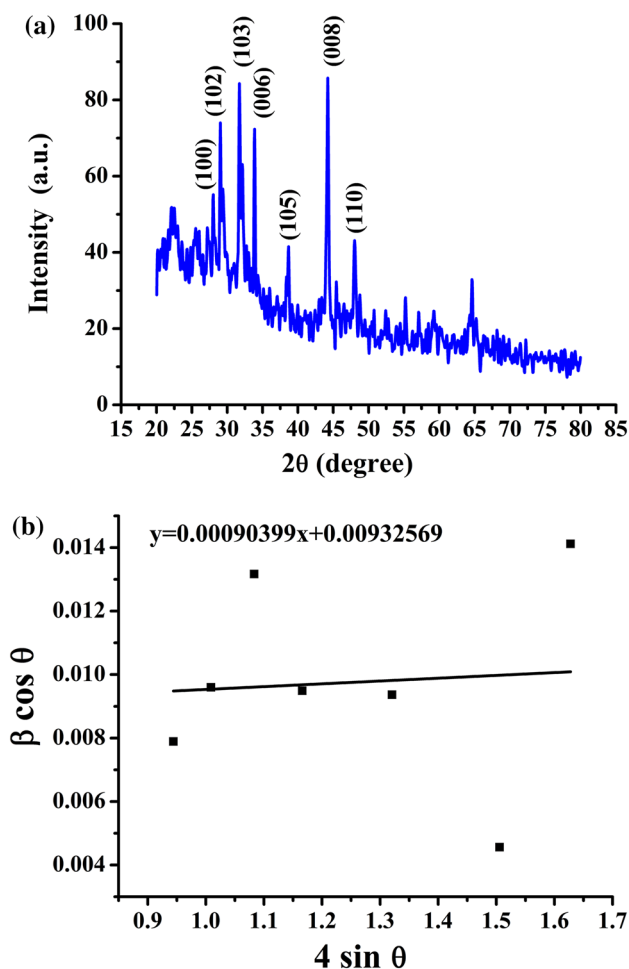


Fig. 2. Structural characteristics of CuS film deposited onto glass substrate (a) XRD and (b) Hall plot; the strain is extracted from the slope, and the crystalline size is extracted from the y-intersect of the fit.

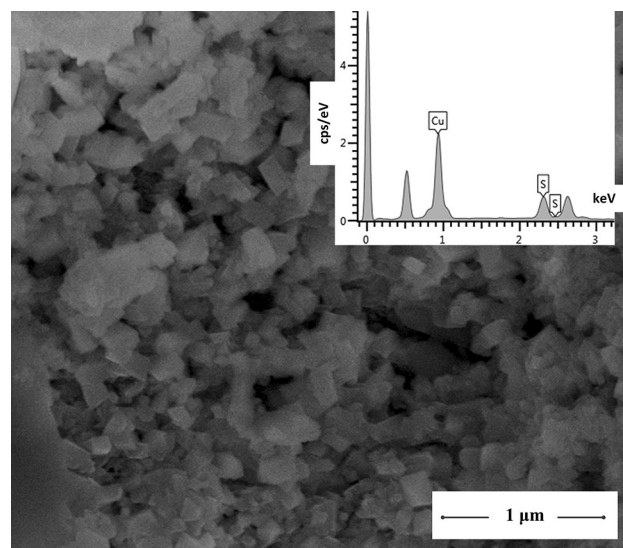


Fig. 3. Morphological characteristics of the CuS membrane.

Table I. The structure parameters of CuS thin film

hkl	2θ (degree)	β_{measured} (degree)	d_{hkl} (nm)	D (nm)
100	27.3053	0.492	0.3266	17.5647
102	29.2199	0.5904	0.3056	14.4404
103	31.4250	0.8	0.2847	10.5245
006	33.8988	0.5904	0.2644	14.6079
105	38.5557	0.5904	0.2335	14.8035
008	44.2270	0.3243	0.2048	30.3873
110	48.0250	0.9	0.1894	9.8159

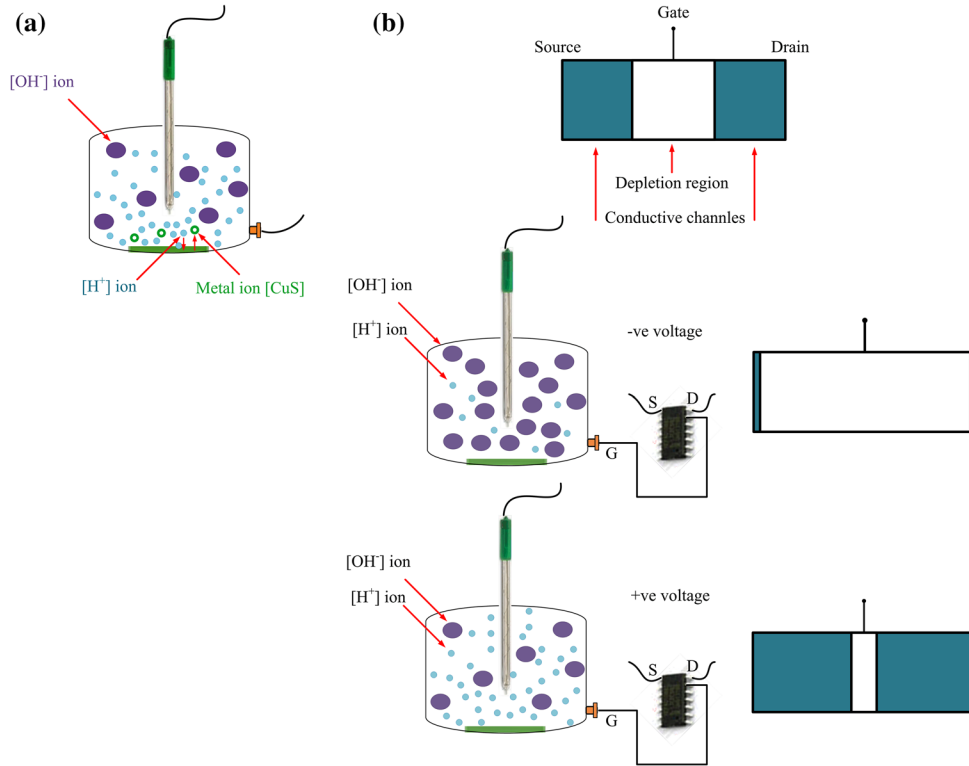
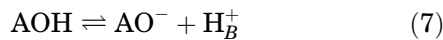
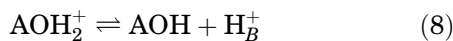


Fig. 4. Schematic of ion behavior: (a) ion exchange between $[H^+]$ and metal $[CuS]$ and (b) mechanism of pH sensitivity with MOSFET.

pH sensitivity. Increasing the number of these sites results in increased potential voltage of the membrane surface, which in turn improves the ion-exchange process that increases the accretion of positive charge on the membrane surface (gate region), subsequently augmenting the pH sensitivity.¹⁷ The principle of pH sensitivity is based on ion exchange between $[H^+]$ ions in the electrolyte and metal ions of EGFET in the membrane surface. The displaced metal ions migrate from the membrane surface into the solution, as shown in Fig. 4a. This ionic exchange is dependent on the type of metal available in the membrane to attract the $[H^+]$ ions. This process controls the pH sensor working mechanism. The site-binding model describes the charging mechanism of an oxide as the equilibrium between the AOH surface sites and the H^+ ions in the bulk of the solution. The surface reactions are expressed as:¹⁸



and



where B refers to the bulk.

The sensitivity parameter β can be estimated with:¹⁷

$$\beta = \frac{2q^2 N_S \sqrt{\left(\frac{K_a}{K_b}\right)}}{kTC_{DL}} \quad (9)$$

where q is the electron charge; N_S indicates the surface site density; K_a and K_b refer to acidic and basic constants, respectively; k denotes the Boltzmann constant; T is the absolute temperature; and C_{DL} describes the capacitance of the electrical double layer.

The membrane sensitivity is dependent on the charge of the surface potential voltage (ψ) between the sensing layer and the electrolyte interface. This is based on site binding theory,¹⁸ which posits that the number of binding sites present in the sensing membrane can change the surface potential voltage between the sensing layer and the electrolyte interface.¹⁷ The surface potential voltage can be explained by:

$$\psi = 2.303 \frac{kT}{q} \frac{\beta}{\beta + 1} (\text{pH}_{PZC} - \text{pH}) \quad (10)$$

where pH_{PZC} refers to the pH value at the point of zero charge. As derived from Eqs. 9 and 10, the sensitivity parameter β relates directly to N_S and the linear response between ψ and the pH value.¹⁷

At the first contact of CuS nanocrystalline structures with an electrolyte, adsorption of $[H^+]$ and $[OH^-]$ occurs (primary adsorption). This process is achieved at a low degree of surface coverage. In addition, the reaction of surface (CuS-OH) groups occurs with $[H^+]$ ions in acidic solution and with $[OH^-]$ ions at basic pH. The rate of this reaction is related to the concentration of free electrons or holes at the surface. This process involves charge

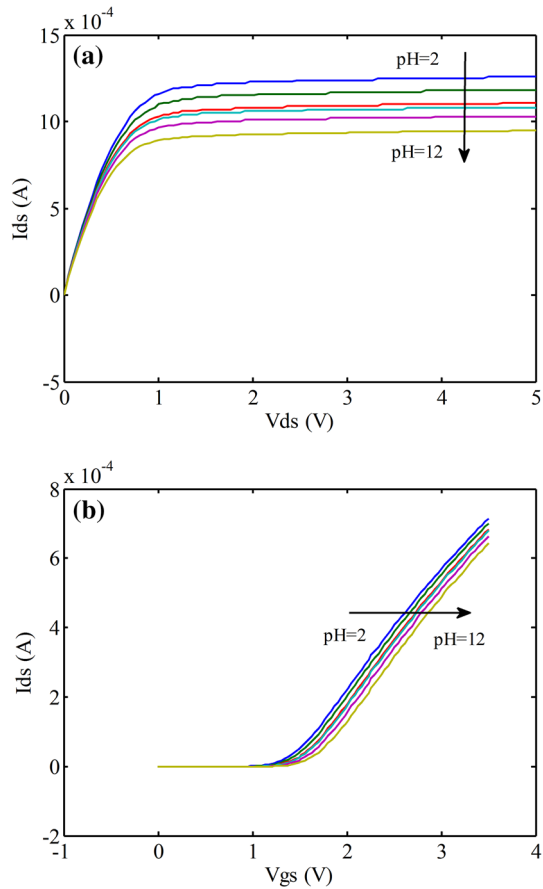


Fig. 5. (I–V) characteristics of the CuS membrane with MOSFET (a) saturation regime and (b) linear regime.

transfer to the solid, which is then distributed by electron transport over the near surface region of the solid to form a depletion layer or to counteract an accumulation layer in acid solution and then to form or enhance an accumulation layer at the base.¹⁶

Sensitivity of CuS Membrane Synthesized With MOSFET

The MOSFET controls the flow of electron (or electron holes) from source (S) to drain (D) by controlling the size and shape of the conductive channel. The channel size controls the positivity ($[H^+]$) or negativity ($[OH^-]$) of the gate-source voltage (V_{gs}). The dependency of I_{ds} on the pH value is a result of the accumulation of $[H^+]$ ions on the sensing surface in the acidic solution, which is equivalent to applying an additional positive voltage at the gate of the MOSFET. This would initiate an increase in the conductive channel with concomitant increase in the current. On the contrary, for the basic solution, the conductive channel becomes constricted or closed when extra negative voltage is applied, thus, decreasing the current as illustrated in Fig. 4b.

The V_{gs} of 3 V was used for ($I_{ds} - V_{ds}$) measurements with a saturation regime, and the V_{ds} of 0.3 V was employed for ($I_{ds} - V_{gs}$) measurements with a linear regime, as shown in Fig. 5. For the saturation regime, the drain-source current (I_{ds}) was found to be inversely proportional to pH, given that I_{ds} shifted downward as the pH increases (alternating from acidic to basic). Conversely, for the linear regime, the threshold voltage (V_{th}), i.e., EGFET turn-on voltage,¹⁷ was found to increase concomitantly with pH. This voltage varies with the surface potential between the membrane surface and the electrolyte. Figure 6 represents the sensitivity of the CuS membrane with MOSFET with values of 29.3 $\mu A/pH$ and 24 mV/pH for the saturation and linear regimes, respectively. Also, the linearity values for the saturation and linear regimes were calculated from Fig. 6 to give values of 97.67% and 98.18%, respectively. The pH solutions used for these measurements were (2–12) step 2. The dependency of V_{th} on the pH value can be illustrated with:¹⁹

$$[H^+]_s = [H^+]_b \exp(-q\phi_0/kT) \quad (11)$$

where the $[H^+]_b$ and $[H^+]_s$ are the bulk and the surface activity of H^+ ions, q is the electron charge, ϕ_0 is the potential on the gate, k is the Boltzmann constant, and T is the absolute temperature. Based on Eq. 11, the decrease of ϕ_0 was found to result in the decrease of output voltage.¹⁹

According to Eq. 11, for acidic solution, the pH has a small value which means a high number of $[H^+]$ ions; hence, the voltage shows a small value. On the other side, when the pH value becomes high for a basic solution according to low $[H^+]$ ions, the threshold voltage increases (shifted to the right), which is illustrated in Fig. 5b.

Sensitivity of CuS Membrane Synthesized Without MOSFET

In the absence of MOSFET, the sensitivity of CuS membranes is measured using the difference between the reference electrode potential and the sensing membrane, by applying the following equation:⁵

$$V_{OUT} = V_{IN}^+ - V_{IN}^- = V_{REF} - V_{SENSING-FILM} \quad (12)$$

where V_{IN}^+ and V_{IN}^- are the two input terminal voltages of the Keithley, and V_{REF} and $V_{SENSING-FILM}$ are the voltages of reference electrode and the sensing film, respectively.

Figure 7a shows the results of the measured voltage with time for pH solutions ranging from 2 to 12. The sensitivity and linearity were calculated to be 22.86 mV/pH and 95.62%, respectively, as shown in Fig. 7b.

According to Eq. 12, in the case of pH 12, which is characterized by a high number of $[OH^-]$ ions and negative voltage, the membrane shows slow or low

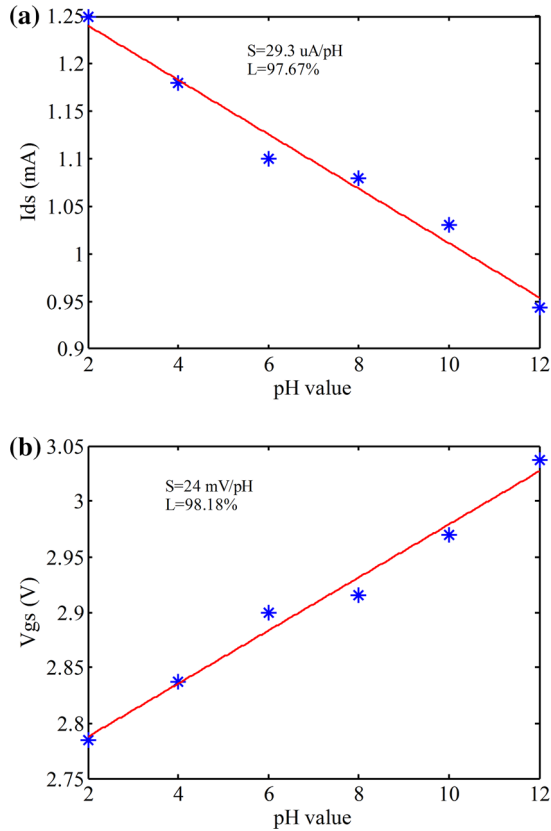


Fig. 6. Sensitivity of the CuS membrane with MOSFET for (a) saturation regime and (b) linear regime.

reaction with the ions of electrolyte because of the limited $[H^+]$ ions and lowered capability of the membrane to exchange metal ions with $[H^+]$ ions. This phenomenon will generate a very small value of $V_{\text{SENSING-FILM}}$ because of the small charge of this membrane, which will result in a large disparity between V_{REF} and $V_{\text{SENSING-FILM}}$, thus, producing high-output voltage. Conversely, for pH 2 with its characteristic higher number of $[H^+]$ and positive voltage, the membrane exhibits rapid or high reaction with the ions of the electrolyte leading to high $V_{\text{SENSING-FILM}}$ because of the large charge present, resulting in a lower difference between V_{REF} and $V_{\text{SENSING-FILM}}$ when compared with the basic solutions. Thus, low-output voltage was obtained for acidic solutions, which is evident in Fig. 7a.

Several membranes^{3,5,20–22} were used as pH sensors with and without MOSFET, and their sensitivities are outlined in Table II.

Hysteresis

Hysteresis is generally associated with the chemical interaction between the $[H^+]$ or $[OH^-]$ ions in the electrolyte and the slow reacting surface sites underneath the membrane surface, referred to as buried sites and/or the defects of the membrane surface. Hysteresis of the CuS membrane, which

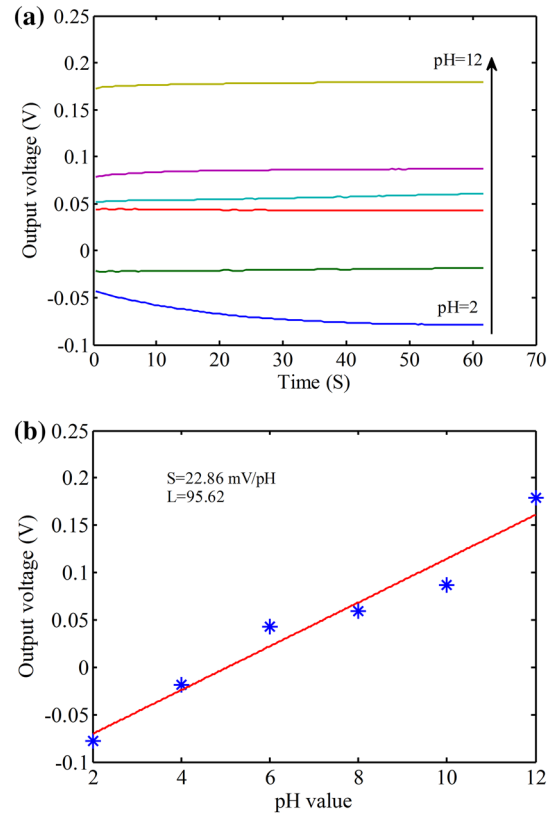


Fig. 7. pH sensitivity of CuS membrane without MOSFET (a) (V–T) characteristics and (b) Sensitivity and linearity.

indicates the defect of the nanocrystals in the membrane surface or underneath the surface, was estimated using Eq. 12. The equation measures the difference between the voltage of the reference electrode and the sensing membrane voltage with time by the setup shown in Fig. 1b. From Fig. 8, a net hysteresis value of 12.8 mV was obtained for the (pH7–pH4–pH7–pH10–pH7) alternating pH cycles when the difference was calculated between the initial and the final output voltage at pH7.⁷ This value is considered to be reasonable when compared with values reported by researchers in related literature. For instance, Yin et al.²⁰ obtained a hysteresis value of 9.8 mV for ITO-sensing EGFET; Das et al.⁷ achieved a hysteresis value of 7.9 mV for PdO-sensing EGFET; and Chiang et al.²³ obtained a hysteresis value of 26 mV for a- WO_3 membrane. A low value of hysteresis denotes the quality of the membrane surface, whereas a high value indicates a delay in pH response as a result of the surface defect of the membrane.

The difference in the interaction behavior for pH4 and pH10 (Fig. 8) can be attributed to the difference in the diffusion rates of $[H^+]$ and $[OH^-]$ ions in the buried sites.^{16, 17,24} $[H^+]$ ions diffused rapidly into the buried sites because of their smaller size when compared with $[OH^-]$ ions, as clearly observed in an alkaline solution of pH10 (Fig. 8). The increased

Table II. pH sensitivity with and without MOSFET for different sensing membranes

Sensing membrane	Method of fabrication	pH solution range	Sensitivity with MOSFET		Sensitivity without MOSFET		Ref.
			(mV/pH)	Linearity (%)	(mV/pH)	Linearity (%)	
SnO ₂	Sputtering	2–12	58	–	56	–	3
SnO ₂	Sputtering	2–12	–	–	59.17	–	23
ITO	–	2–12	58	–	57	–	20
AZO	Hydrothermal growth method	1–13	57.95	0.9998	–	–	5
TiN	Thermal evaporation	1–12	–	–	56.3	–	24
CuS	Spray pyrolysis deposition	2–12	24	98.18	22.86	95.62	This work

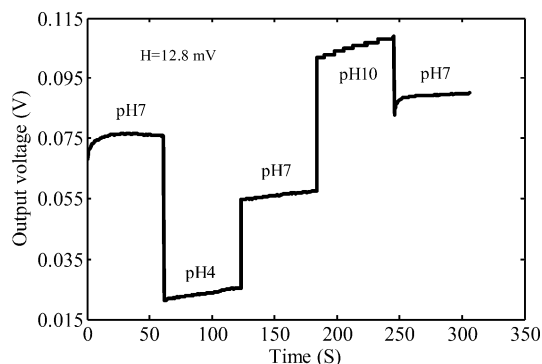


Fig. 8. Hysteresis of the CuS membrane.

drift is attributable to the permeation of $[\text{OH}^-]$ ions through the CuS nanocrystalline film to form buried sites that react slowly as a result of the indolent ionic diffusion throughout the electrolyte–membrane–surface interface. Hence, the hysteresis is more important in an alkaline solution.^{17,24} This explanation is consistent with the hysteresis values of 8.2 mV and 10.5 mV measured in low and high loop pH, respectively, for porous silicon EGFET¹⁷; values of 35.1 μA and 73.6 μA in low and high loop pH, respectively, for TiO₂/ITO EGFET²⁴; and values of 20.7 mV and 30.9 mV in low and high loop pH, respectively, for CuS EGFET.

CONCLUSION

The hysteresis and sensitivity of the CuS membrane, in the presence and absence of MOSFET, were investigated. The CuS membrane was prepared with deionized water and subsequently deposited on a glass substrate via spray pyrolysis deposition. Afterward, the CuS membrane was tested as a pH sensor. The results showed that MOSFET improved the sensitivity (24 mV/pH) of the thin film. In addition, EGFET exhibited comparably higher stability because the MOSFET was not dipped in the buffer solution. The results also revealed that MOSFET is influenced by the gate-source voltage, which can increase or decrease the

drain-source current, thereby influencing the sensitivity of the pH sensor. A reasonable hysteresis value of 12.8 mV was obtained for the CuS membrane. Based on the characterization results, it can be inferred that the nanocrystallinity of the CuS membrane plays a significant role in the improvement of its pH-sensing capability because of its nanoscale and high surface-to-volume ratio.

ACKNOWLEDGEMENT

The authors gratefully acknowledge the financial support of the University Sains Malaysia and the RU Top-Down Grant 1001/CINOR/870019.

REFERENCES

1. E.M. Guerra and M. Mulato, *J. Sol-Gel. Sci. Technol.* 52, 315 (2009).
2. P. Bergveld, *IEEE Trans. Biomed. Eng BME* 17, 70 (1970).
3. L.-L. Chi, J.-C. Chou, W.-Y. Chung, T.-P. Sun, and S.-K. Hsiung, *Mater. Chem. Phys.* 63, 19 (2000).
4. T. Matsuo and M. Esashi, *Sensor Actuat.* 1, 77 (1981).
5. J.-L. Wang, P.-Y. Yang, T.-Y. Hsieh, C.-C. Hwang, and M.-H. Juang, *J. Nanomater.* Article ID 152079, 7 (2013).
6. S.X. Chen, S.P. Chang, and S.J. Chang, *Dig J. Nanomater. Biostruct.* 9, 1505 (2014).
7. A. Das, D.H. Ko, C.-Hsin Chen, L.-Be Chang, C.-Sung Lai, F.-Chuan Chu, L. Chow, and R.-Ming Lin, *Sensor Actuat. B-Chem.* 205, 199 (2014).
8. H.-H. Lu, W.-S. Dai, J.-C. Chou, and H.-C. Cheng, *IEEE Electron. Device Lett.* 33, 1495 (2012).
9. K. Anuar, W.T. Tan, N. Saravanan, L.K. Khor, and S.M. Ho, *J. Nepal Chem. Soc.* 25, 2 (2010).
10. M. Lee and K. Yong, *IOP Publish. Nanotech.* 23, 194014 (2012).
11. A.D. Dhondge, S.R. Gosavi, N.M. Gosavi, C.P. Sawant, A.M. Patil, A.R. Shelke, and N.G. Deshpande, *WJCM* 5, 1 (2015).
12. X.L. Yu, Y. Wang, H.L.W. Chan, and C.B. Cao, *Micropor. Mesopor. Mater.* 118, 423 (2009).
13. K.D. Yuan, J.J. Wu, M.L. Liu, L.L. Zhang, F.F. Xu, L.D. Chen, and F.Q. Huang, *Appl. Phys. Lett.* 93, 132106 (2008).
14. R. Das and S. Sarkar, *Mater. Chem. Phys.* 167, 97 (2015).
15. A.K. Zak, W.H.A. Majid, M.E. Abrishami, and R. Yousefi, *Solid State Sci.* 13, 251 (2011).
16. S.A.-Hilli, M. Willander, *Sensors* 9, 7445 (2009).
17. N.H. Al-Hardan, M.A.A. Hamid, N.M. Ahmed, A. Jalar, R. Shamsudin, O.K. Othman, L.K. Keng, W. Chiu, and H.N. Al-Rawi, *Sensors* 16, 839 (2016).
18. D.E. Yates, S. Levine, and T.W. Healy, *J. Chem. Soc., Faraday Trans.* 70, 1807 (1974).

19. P.-Y. Chen, L.-T. Yin, T.-H. Cho, *Life Sci. J.* 11, 871 (2014).
20. L.-T. Yin, J.-C. Chou, W.-Y. Chung, T.-P. Sun, S.-K. Hsiung, *Mater. Chem. Phys.* 70, 12 (2001).
21. C.-W. Pan, J.-C. Chou, T.-P. Sun, S.-K. Hsiung, *Sensor. Actuat. B-Chem.* 108, 863 (2005).
22. S.S.K. Hsiung, J.-C. Chou, T.-P. Sun, W.-Y. Chung, Y.-L. Chin, L. Z. Ce, Patent Application Publication US, 2004/0185591 A1 (2004).
23. J.L. Chiang, S.S. Jan, J.C. Chou, Y.C. Chen, *Sensor Actuat. B-Chem.* 76, 624 (2001).
24. P.-C. Yao, J.-L. Chiang, M.-C. Lee, *Solid State Sci.* 28, 47 (2014).